Original Article

MOLECULAR METABOLISM

Dietary sugars, not lipids, drive hypothalamic inflammation

Yuanqing Gao [1,2,12], Maximilian Bielohuby [3,12], Thomas Fleming [4], Gernot F. Grabner [5], Ewout Foppen [2], Wagner Bernhard [6], Mara Guzmán-Ruiz [7], Clarita Layritz [1], Beata Legutko [1], Erwin Zinser [6], Cristina García-Cáceres [1], Ruud M. Buijs [7], Stephen C. Woods [8], Andries Kalsbeek [2,9], Randy J. Seeley [10], Peter P. Nawroth [4], Martin Bidlingmaier [3,***], Matthias H. Tschöp [1,11,**], Chun-Xia Yi [2,*]

ABSTRACT

Objective: The hypothalamus of hypercaloric diet-induced obese animals is featured by a significant increase of microglial reactivity and its associated cytokine production. However, the role of dietary components, in particular fat and carbohydrate, with respect to the hypothalamic inflammatory response and the consequent impact on hypothalamic control of energy homeostasis is yet not clear.

Methods: We dissected the different effects of high-carbohydrate high-fat (HCHF) diets and low-carbohydrate high-fat (LCHF) diets on hypothalamic inflammatory responses in neurons and non-neuronal cells and tested the hypothesis that HCHF diets induce hypothalamic inflammation via advanced glycation end-products (AGEs) using mice lacking advanced glycation end-products (AGEs) receptor (RAGE) and/or the activated leukocyte cell-adhesion molecule (ALCAM).

Results: We found that consumption of HCHF diets, but not of LCHF diets, increases microgliosis as well as the presence of N(ε)-(Carboxymethyl)-Lysine (CML), a major AGE, in POMC and NPY neurons of the arcuate nucleus. Neuron-secreted CML binds to both RAGE and ALCAM, which are expressed on endothelial cells, microglia, and pericytes. On a HCHF diet, mice lacking the RAGE and ALCAM genes displayed less microglial reactivity and less neovasculature formation in the hypothalamic ARC, and this was associated with significant improvements of metabolic disorders induced by the HCHF diet.

Conclusions: Combined overconsumption of fat and sugar, but not the overconsumption of fat *per se*, leads to excessive CML production in hypothalamic neurons, which, in turn, stimulates hypothalamic inflammatory responses such as microgliosis and eventually leads to neuronal dysfunction in the control of energy metabolism.

Keywords Microglia; POMC; Obesity; Pericytes; Angiogenesis

1. INTRODUCTION

Containing highly heterogeneous neuronal and glial populations that receive and integrate diverse metabolic feedback signals from the periphery, the hypothalamus is key for metabolic sensing and regulation. Accumulating evidence points to disrupted hypothalamic functioning as a major player in hypercaloric diet-induced obesity and associated metabolic disorders [1–3]. The hypothalamus of hypercalorically diet-induced obese animals is characterized by an increased inflammatory response, reflected in part by a significant increase of microglial reactivity, particularly in the area of the arcuate nucleus (ARC), i.e., the nucleus that contains the anorexigenic pro-

[1]Institute for Diabetes and Obesity, Helmholtz Diabetes Center (HDC), Helmholtz Zentrum München and German Center for Diabetes Research (DZD), München-Neuherberg, Germany [2]Department of Endocrinology and Metabolism, Academic Medical Center, University of Amsterdam, The Netherlands [3]Endocrine Research Unit, Klinikum der Ludwig-Maximilians-Universität, Munich, Germany [4]Department of Medicine and Clinical Chemistry, University Hospital of Heidelberg, Germany [5]Institute of Molecular Biosciences, University of Graz, Austria [6]FH JOANNEUM University for Applied Sciences, Graz, Austria [7]Universidad Nacional Autónoma de México, Mexico [8]Institute for Metabolic Diseases, University of Cincinnati, USA [9]Hypothalamic Integration Mechanisms, Netherlands Institute for Neuroscience, Amsterdam, The Netherlands [10]Department of Surgery, University of Michigan, USA [11]Division of Metabolic Diseases, Technische Universität München, Munich, Germany

[12] Yuanqing Gao and Maximilian Bielohuby contributed equally to this work.

*Corresponding author. Department of Endocrinology and Metabolism, Academic Medical Center, University of Amsterdam, Meibergdreef 9, 1105 AZ, Amsterdam, The Netherlands. Fax: +31 20 6917682. E-mail: c.yi@amc.uva.nl (C.-X. Yi).

***Corresponding author. Medizinische Klinik und Poliklinik IV, Klinikum der Universität München, Ziemssenstr. 1, 80336, Munich, Germany. Fax: +49 89 4400 54457. E-mail: martin.bidlingmaier@med.uni-muenchen.de (M. Bidlingmaier).

**Corresponding author. Helmholtz Diabetes Center, Helmholtz Zentrum München, Parkring 13, 85764, Neuherberg, Germany. Fax: +49 89 31872182. E-mail: tschoep@helmholtz-muenchen.de (M.H. Tschöp).

Received April 1, 2017 • Revision received June 8, 2017 • Accepted June 14, 2017 • Available online 20 June 2017

http://dx.doi.org/10.1016/j.molmet.2017.06.008

opiomelanocortin (POMC) and the orexigenic agouti-related peptide (AgRP)/neuropeptide Y (NPY) neurons. The increase of microglial reactivity is accompanied by astrocytosis and *de novo* angiogenesis, and, in the long run, leads to the loss of POMC neurons [2–4].

In hypercaloric diet-induced obesity, dietary fats, and especially saturated fatty acids, are considered to be the essential component initiating pro-inflammatory responses in the hypothalamus [5]. However, the role of dietary carbohydrates with respect to the hypothalamic inflammatory response and the consequent impact on hypothalamic control of energy homeostasis is not yet clear. In the current series of mouse and rat studies, we documented that the mediobasal hypothalamic inflammatory response occurs in response to high-fat diets rich in carbohydrates (high-carbohydrate high-fat (HCHF) diets), but not in response to a low-carbohydrate, high-fat (LCHF) diet. This HCHF-induced mediobasal hypothalamic inflammatory response was mediated by advanced glycation end products (AGEs) produced by hypothalamic neurons acting on microglia, endothelial cells, and pericytes that express AGE receptors. Genetic deletion of AGE receptors in mice fed a HCHF diet resulted in less microglial reactivity and less angiopathy in the hypothalamic ARC than in their WT controls, as well as reducing the severity of the metabolic disorders induced by the HCHF diet.

2. MATERIALS AND METHODS

2.1. Animals

All rodent studies were approved by and performed according to the guidelines of the Institutional Animal Care and Use Committee of the Helmholtz Center Munich, or the University of Cincinnati. Male mice and rats were housed on a 12-h light, 12-h dark cycle (light from 7 am to 7 pm) at 22 °C with free access to food and water. Generation of receptor of advanced glycation end products KO ($RAGE^{-/-}$) mice is described elsewhere [6]; activated leukocyte cell adhesion molecule KO ($ALCAM^{-/-}$) mice, $POMC^{eGFP}$ and NPY^{eGFP} mice were purchased from the Janvier (Le Genest-Saint-Isle, France) or Jackson Laboratory (Bar Harbor, ME, USA) with the C57BL/6 genetic background. RAGE and ALCAM double-knockout mice were generated by cross-breeding $ALCAM^{-/-}$ and $RAGE^{-/-}$ mice. Diets were custom designed and purchased from Provimi Kliba Nafag (Kaiseraugst, Switzerland) or purchased from *Research Diet* (D12331). Body weight and food intake were monitored according to each experimental design.

Whole body composition was measured using NMR technology (EchoMRI, Houston, TX). Fat and lean body mass were calculated as a percentage of total body weight.

2.2. Glucose tolerance test

Intraperitoneal glucose tolerance tests were performed for the determination of the effects of deletion of RAGE and ALCAM genes on glucose metabolism in mice fed chow or HCHF diet. Mice were fasted for 6 h (8:00 to 14:00), and tail blood glucose level was measured before (t = 0) and after intraperitoneal glucose injection (2 g/kg BW) at t = 15, 30, 60, and 120 min, by using a handheld glucometer (TheraSense FreeStyle).

2.3. CML infusion into mediobasal hypothalamus

For CML infusion into the MBH, with a standard Kopf stereotaxic apparatus, bilateral infusion probe was placed into the top of the arcuate nucleus in the brain of Wistar rats (AP: −3.14 mm, L: 0.6 mm, V: −9.8 mm) (average body weight of rats is 300 g). After recovery, artificial cerebral fluid (aCSF, as vehicle) or CML (5 μg in 2 μl aCSF) was infused via the probe into the MBH, once per day, in 7 consecutive days. Rats were sacrificed by perfusion fixation 4 h after last infusion.

2.4. Immunohistochemical and immunofluorescent staining

For immunohistochemical and immunofluorescent staining, mice and rats were rapidly euthanized in CO2 and transcardially perfused with phosphate-buffered saline (PBS) followed by 4% neutral buffered paraformaldehyde (Fisher Scientific). Brains were extracted, equilibrated in 30% sucrose, sectioned coronally on a cryostat (Leica Biosystems) at 30 μm and collected and rinsed in 0.1 M TBS. Mouse brains for vessel length measurement by the FITC-albumin infusion approach were prepared by emulsion fixation with 4% paraformaldehyde after receiving FITC-albumin (Sigma-Aldrich, St. Louis, MO, USA) infusion, sucrose equilibration and sectioning.

2.4.1. Immunohistochemical staining

Brain sections were incubated with primary antibody of rabbit anti-iba1 (1:1500, Synaptic Systems, Germany), rabbit anti-GFAP (1:2000, DAKO, Germany), rabbit anti-PDGFRβ (1:500, Abcam, USA), or rabbit anti-CML (1:500, Abcam, USA). Primary antibodies were incubated overnight at 4 °C. Sections were rinsed and incubated in biotinylated secondary goat anti-rabbit IgG; sections were then rinsed and incubated in avidin-biotin complex (ABC method, Vector Laboratories, Inc., Burlingame, CA) for 1 h, and the reaction product was visualized by incubation in 1% diaminobenzidine with 0.01% hydrogen peroxide for 5–7 min. Sections were mounted on gelatin-coated glass slides, dried, dehydrated through a graded ethanol series, cleared in xylene, and cover-slipped for image collection and quantification. For image analysis, microscope: Zeiss AXIO Scope A1, objective lenses: Plan-APOCHROMAT 10X/0.45, Camera: Zeiss, AxioCam MRc, Acquisition software: AxioRel Vision 4.8. Imaging quantification was performed blinded; cell numbers were manually counted within a framed area inside the ARC. The coverage of the iba1-ir and GFAP-ir positive cells, and the integrative density of CML-ir cells was measured by ImageJ. For measurement of cell coverage, 8-bit images collected from iba1 and GFAP staining were processed into binary pictures, and the area covered by the immunoreactive cells and their processes was measured. For microglia, the total area of coverage was then divided by the number of iba1-ir microglia counted in the same area in the ARC, to obtain the data for iba1-ir coverage per cell. For astrocytes, data of the total coverage area were presented.

2.4.2. Immunofluorescent staining

For detecting the colocalization of CML with GFP (in $Pomc^{eGFP}$ or Npy^{eGFP} mice, in which GFP can be visualized directly by fluorescent microscope), brains sections were incubated with rabbit anti-CML (1:200) primary antibody overnight at 4 °C as described above. Sections were rinsed and incubated with biotinylated secondary horse anti-rabbit IgG for 1 h, and then rinsed and incubated with streptavidin-conjugated Alexa Fluor® 594 or 647 (Jackson ImmunoResearch, USA) for 1 h. For detecting the colocalization of CML with NeuN or GFAP, brains sections were incubated with primary antibodies of rabbit anti-CML (1:200), in combination with mouse anti-NeuN (1:200) or goat anti-GFAP (1:500. Abcam, USA) overnight at 4 °C as described above. Sections were rinsed and incubated with biotinylated secondary horse anti-rabbit IgG for 1 h, and then rinsed and incubated with streptavidin-conjugated Alexa Fluor® 594 or 647, in combination with goat anti-mouse IgG-conjugated Alexa Fluor® 647 or donkey anti-goat IgG-conjugated Alexa Fluor® 594 (Jackson

ImmunoResearch, USA) for 1 h. For detecting the colocalization of GFP (in RAGE$^{-/-}$ or ALCAM$^{-/-}$ mice, in which GFP can be detected by anti-GFP antibody) with laminin, iba1, PDGFRβ, NeuN, POMC, CML, and GFAP, brain sections were incubated with goat anti-GFP (1:200), in combination with one of the primary antibodies: chicken anti-laminin (1:1000, Abcam, USA), rabbit anti-iba1 (1:300), rabbit anti-PDGFRβ (1:200), mouse anti-NeuN (1:200, Milipore), rabbit anti-POMC (1:300, Phoenix Pharmaceuticals, USA), rabbit anti-GFAP (1:1000), or rabbit anti-CML (1:200) was incubated overnight at 4 °C as described above. Next, sections were rinsed and incubated with biotinylated secondary donkey anti-goat IgG for 1 h; sections were then rinsed and incubated with streptavidin-conjugated Alexa Fluor® 488 or 594 (Jackson ImmunoResearch, USA) in combination with goat anti-rabbit IgG-conjugated Alexa Fluor® 488, 594 or 647, goat anti-chicken IgG conjugated Alexa Fluor® 594, or goat anti-mouse conjugated Alexa Fluor® 594 for 1 h. All sections were then rinsed and mounted on gelatin-coated glass slides, dried, covered with polyvinyl alcohol mounting medium containing DABCO® (Sigma, USA), observed and imaged by confocal microscopy (Leica SP5, Germany). For image analysis, microscope: Leica TCS SP5 II, objective lenses: HCX PL APO, 63x, NA=1.3, Imaging medium: Glycerol, Fluorochromes: Alexa 488, 594 & 647, Camera: Leica TCS SP5 II, Acquisition software: LAS AF, image processing: IMARIS7.6.4 (Bitplane, UK). Mouse brains for vessel length measurement by Fluorescein (FITC)-albumin infusion approach were performed as described before. For vascular density analysis, images were skeletonized before histogram analysis [4].

2.5. Western blot analysis

Tissues from the mediobasal hypothalamus (MBH) of Chow, HCHF1, HCHF2, LCHF1, and LCHF2 diet-fed mice were snap frozen for detection of two major AGEs modified proteins — the CML-modified proteins and the methylglyoxal (MG-H1)-modified proteins. The CML and MG(-H1) antibodies were generated by the Nawroth lab using non-reactive peptide antigens that contain the modification in a specific location. The specificity for the modification was tested using similar chemical-defined peptides and in both cases the specificity is 100% for CML or MG-H1. Neither of the antibodies showed any reactivity for any other AGEs. After protein extraction, protein concentration was determined by BCA assay. The same amount of protein from lysates was placed in 1.5-mL tubes. 4× NuPAGE LDS Sample Buffer (Invitrogen) was added to each and incubated at 95 °C for 5 min. After heating, the mixture was kept on ice for 20 min. Twenty μg protein lysates from each sample were then separated by 10% precast gel (Bio-Rad), and transferred to nitrocellulose membranes (Bio-Rad). After the transfer, the membranes were blocked in non-protein blocking buffer (Thermo Scientific, to prevent AGEs contamination) for 1 h. Primary antibodies (rat anti-MG-H1 monoclonal antibody, 10 μg/ml) were diluted in non-protein blocking buffer and incubated with the membrane overnight at 4 °C. On the following day, membranes were washed by Tris-buffered saline with Tween (TBST) three times for 10 min and incubated with the HRP conjugated secondary antibody for 1 h at room temperature and washed again in TBST (three times for 10 min). Membranes were then developed by ECL (Bio-Rad) and imaged with Odyssey imaging system (LI-COR Bioscience). The blots with anti-CML and anti-beta-actin were performed consecutively after the membrane from MG-H1 blotting was stripped and incubated with either mouse anti-CML monoclonal antibody (0.25 mg/ml) or rabbit anti-beta-actin (Cell Signaling).

2.6. CML treating hypothalamic microglia

For CML treatment of hypothalamic microglia, primary cultured hypothalamic microglia were obtained from dissected hypothalamus on postnatal day 2 and cultured by a method adapted from Saura et al. [7]. Seventeen days afterward, cells received serum starvation for 5 h and were treated with CML (50 μM) or vehicle for 16 h. Microglia were then snap frozen in liquid nitrogen for gene or protein expression analysis.

2.7. Far-western blotting analysis

Far-Western blotting analysis was executed as described before [8]. Briefly, 2 μg recombinant CD166/ALCAM protein (Recombinant Mouse ALCAM/CD166 Fc Chimera; R&D Systems) and RAGE protein (Recombinant Mouse RAGE Fc Chimera R&D Systems) were separated on 10% SDS gels (Bio-rad cat.567-1033) and transferred to PVDF membranes. Membranes were then incubated with AC buffer (100 mM NaCl, 20 mM Tris [pH 7.6], 0.5 mM EDTA, 10% glycerol, 0.1% Tween-20, and 1 mM DTT) containing guanidine-HCl 6 M, 3 M, 1 M for 30 min at room temperature, followed by AC-buffer (guanidine-HCL 0.1 M and 0 M) at 4 °C for 30min and 1 h, respectively, and finally blocked with protein free blocking buffer (Fisher Scientific Cat. No.10269613) for 1 h at room temperature. Membranes were then incubated with 1.5μM of CML-human serum albumin (HSA) or lysine (as vehicle control, Sigma, cat. No.L5551) in protein-binding buffer (100 mM NaCl, 20 mM Tris [pH 7.6], 10% glycerol, 0.1% Tween-20, 1 mM DTT, 4 mM $CaCl_2$) overnight at 4 °C. On the following day, membranes were washed four times with TBS with Tween 20(0.1%) and then incubated with anti-CML Ab (Rabbit anti-CML, Abcam) diluted 1:1000 in blocking buffer with 4 mM $CaCl_2$ overnight at 4 °C. After washing, secondary antibodies (goat anti rabbit IgG, Santa Cruz, sc-2004) were added at 1:2000 in blocking buffer and incubated with membranes for 1 h at room temperature. Membranes were developed by same methods as Western Blotting.

2.8. Gene expression analysis by real-time PCR

Microglia treated by CML and MBH tissues isolated from chow or HCHF1 diet-fed mice were snap frozen in liquid nitrogen. Total RNA was isolated and purified with RNeasy Mini Kit (QIAGEN). cDNA was synthesized by Superscript III 1st Strand Synthesis Kit (Invitrogen). Real-time PCR was applied with TaqMan® probes (Applied Biosystems). NCBI reference sequences of the target genes for RT-PCR are TNF-alpha: NM013693, IL-1beta: NM008361.3, RAGE: NM001271422.I, ALCAM: NM009655.2, HPRT: NM013556.2. Expression levels of each gene were normalized to housekeeping genes HPRT, relative expression of the targeted gene was presented as fold change compared to the control group that was set at 1.

2.9. Analytical methods

For measuring hypothalamic eicosanoids and sterols, mice were euthanized in CO2 rapidly and transcardially perfused with PBS to flush out blood, MBH tissues were then isolated and snap frozen in liquid nitrogen. Hypothalamic eicosanoids and sterols were measured by liquid-chromatography — mass spectrometric (LC-MS) method [9].

2.10. Statistics

All data are expressed as means ± s.e.m. Statistical analyses were performed using Prism5.0 (GraphPad). Two tailed Student *t*-test, one-way, or two-way analysis of variance (ANOVA) were used to test for differences between individual experimental groups.

3. RESULTS

3.1. A high-carbohydrate, high-fat diet, but not low-carbohydrate, high-fat diet, induces obesity and increases the hypothalamic inflammatory response.

To dissect the effects of fat and carbohydrates in a hypercaloric diet on hypothalamic microglial activity, we fed 10 weeks old WT mice either a standard chow diet, which is a low-fat, high-carbohydrate diet, or one of the following four high-fat diets with either high or low amounts of carbohydrate and ample protein (Table 1). The two high-carbohydrate, high-fat diets contained either sucrose (HCHF1) or starch (HCHF2) as the carbohydrate source. The two low-carbohydrate, high-fat diets were a non-ketogenic Atkins-style diet (LCHF1), as is often used for dieting purposes with very low carbohydrate content but normal protein and high in fat [10,11], and a ketogenic low-carbohydrate, high-fat diet (LCHF2). The fats in the HCHF1 diet were soybean oil and coconut oil, the fat in the HCHF2, LCHF1, and LCHF2 diet was beef tallow [12]. Moreover, LCHF2 has lower dietary protein content as compared to LCHF1 and this type of diet is often used for treatment of pediatric epilepsy [11,13,14]. All five diets were fed *ad libitum* for 4 wk.

In comparison to the chow group, all four HF diet groups had significantly higher daily caloric intake, being highest in the HCHF2 group (Figure 1A). HCHF1 and HCHF2 groups equally gained the most BW in each of the 4 wk, while the LCHF1 group gained less, the difference reaching statistical significance vs. chow in wk4 (Figure 1B and C, Supplemental Figure 1A). In contrast, mice fed with LCHF2 lost BW in all 4 wk. Compared to the chow group, all four HF diet groups gained significantly more fat mass (Figure 1D, Supplemental Figure 1B) and thus had proportionally less lean mass than the chow group (Supplemental Figure 1D and E). Plasma leptin levels of all HF diets group were increased and reached significance in HCHF1, HCHF2, and LCHF2 diet groups; moreover, the leptin level in the LCHF2 group was significantly lower than that in the HCHF1 and HCHF2 groups (Supplemental Figure 1C).

To investigate dietary impact on CNS components of the systemic meta-inflammation known to associate with obesity, we evaluated hypothalamic microglial and astrocyte activities after 4 wk. Mice fed either HCHF diet had significantly increased cell number of the microglial activity marker, ionized calcium-binding adapter molecule 1 (iba1-ir) in the ARC (Figure 1E and I). Furthermore, the HCHF1 and HCHF2 groups had the highest level of cell coverage of iba1-ir microglia (Figure 1 F), and although LCHF1 also showed an increase, it was significantly lower than that of the two HCHF groups. Similar findings between LCHF1 and LCHF2 groups point toward a minor role of the dietary protein content in HF diets with respect to hypothalamic microglial and astrocyte activities. The changes in iba1-ir were not associated with the hypothalamic eicosanoids or sterols that have been reported to be important inflammatory mediators in peripheral tissues [15] (Supplementary Figures 2 and 3). Thus, although mice fed the LCHF diets consumed a similar high amount of fat as the HCHF mice, the lack of carbohydrates in the diets was associated with hypothalamic microglia remaining in a quiescent state. Intriguingly, the immunoreactivity of the astrocytic marker, glial fibrillary acidic protein (GFAP-ir), significantly increased in all four high-fat diets groups (Figure 1G and J). Thus, in a hypercaloric environment, a high amount of dietary fat *per se* seems to be a prerequisite to influence hypothalamic astrocytic reactivity.

Table 1 — Diet components and metabolizable energy.

Diet composition	Fat (%)	Protein (%)	Carbohydrate (%)	Metabolizable energy (Mcal/kg)
High carbohydrate low fat (Chow)	16.7	19	64.3 (wheat & corn)	3.84
High carbohydrate high fat (HCHF1)	58.0	16.5	25.5 (sucrose)	5.56
High carbohydrate high fat (HCHF2)	61.9	18.7	19.4 (starch)	5.08
Low carbohydrate high fat (LCHF1)	78.7	19.1	2.20	6.17
Low carbohydrate high fat (LCHF2)	92.8	5.5	1.70	7.20

3.2. A HCHF diet increases N-epsilon-(carboxymethyl)lysine content in POMC and NPY neurons in the ARC

The association between the two HCHF diets, but not between the two LCHF diets, and the ARC microglial reactivity raised the question of which non-high-fat factors are involved in the HCHF-induced microglial activation. It is known that advanced glycation end products (AGEs) are modifications of proteins that become non-enzymatically glycated and oxidized after contact with aldose sugars [16]. Increased levels of AGEs in hyperglycemic conditions in diabetes are believed to play a major role in vascular pathogenesis. To investigate whether the HCHF diet-induced-hypothalamic inflammatory response is associated with AGEs in the ARC, we measured the content of one of the major types of AGEs, N-epsilon-(carboxymethyl)lysine (CML), that can be produced by both glycoxidation and lipoxidation reactions [17]. First of all, among different cell populations in the mediobasal hypothalamus, we found that CML-ir was only observed in neurons (Supplementary Figure 4A), and not in iba1-ir microglia, GFAP-ir astrocytes, or endothelial cells (Supplementary Figure 4B—D). Secondly, in comparison to the chow group, all four high-fat diet groups contained significantly more CML immunoreactivity (CML-ir) in the ARC (Figure 1H and K). The HCHF1 and HCHF2 groups had significantly more CML-ir than the LCHF1 and LCHF2 groups, indicating that the combination of high fat and high carbohydrate has the greatest impact on CML content in the hypothalamic ARC. Consistent with the increased CML-ir in the ARC, we also detected increases of a variety of CML-modified proteins in the HCHF1 and/or HCHF2 diet-fed mouse hypothalami (Supplementary Figure 5A). Furthermore, we also found significant increases of another major AGE species — the methylglyoxal (MG-H1) modified proteins — in the HCHF1 and/or HCHF2 diet-fed mouse hypothalamus (Supplementary Figure 5B), suggesting a general increase of major AGEs species on HCHF diets.

No significant differences were identified between the HCHF1 and HCHF2 diets in terms of their impacts on food intake, BW, hypothalamic iba1-ir, and CML-ir, implying that there were no major differences between sucrose-derived and starch-derived carbohydrates regarding their effects on obesity and the hypothalamic inflammatory response. Therefore, in the following experiments, we used the HCHF1 diet to assess the impact of CML on energy metabolism.

To further examine the CML content in POMC and NPY neurons in the ARC, we fed POMC-EGFP or NPY-EGFP promoter transgenic mice with HCHF1 diet for one month and compared them to mice that were fed chow. On chow, both POMC and NPY neurons contained CML-ir (18% of POMC neurons and 24% of NPY neurons) (Figure 2A, C and E). After 4 wk of HCHF diet, CML-ir was significantly increased in both POMC (49%) and NPY neurons (45%) (Figure 2B, D and E), implying that the HCHF diet has a similar impact on stimulating CML production in both POMC and NPY neurons.

3.3. Hypothalamic non-neuronal cells express receptors for AGEs

AGEs induce tissue dysfunction by receptor-dependent mechanisms [18]. By far-western blotting analysis, we found that CML binds to the

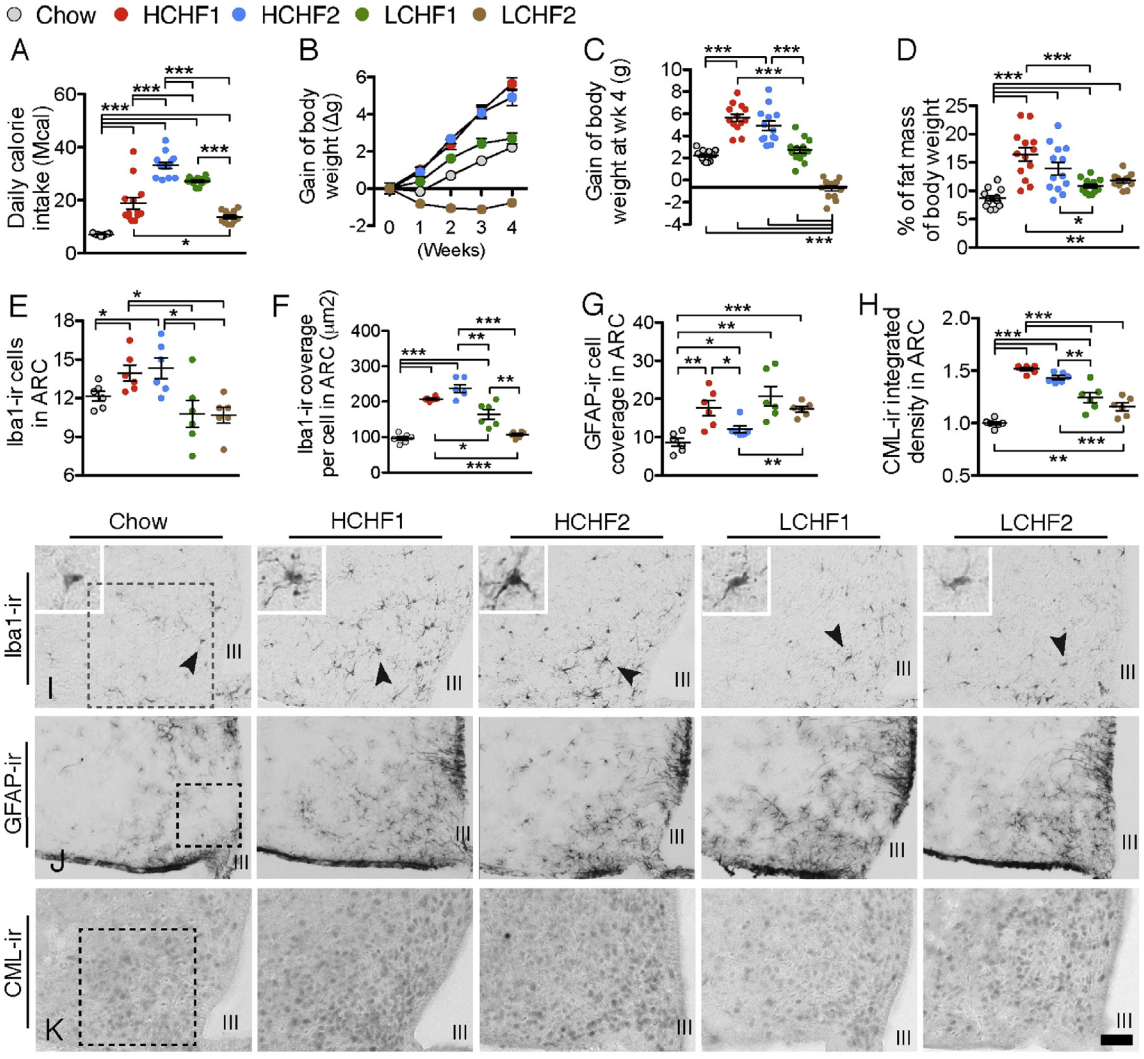

Figure 1: High carbohydrate, high fat diets, but not low-carbohydrate, high-fat diets, increase hypothalamic microglial reactivity and neuronal CML content. (**A**) Daily calorie intake of chow, HCHF1, HCHF2, LCHF1, and LCHF2 diet groups (n = 13 for each group, F(1,60) = 80.26, P < 0.0001). (**B** & **C**) Independent of daily calorie intake, the HCHF1 and HCHF2 groups had the most profound impact on BW gain (n = 13 for each group). (**D**) Fat mass proportion of total BW of each diet group (n = 13 for each group). (**E**) Quantification of the number of iba1-ir microglia in a frame of 0.2 mm × 0.2 mm in the ARC (illustrated in I) from each diet group (n = 6 for each group). (**F**) Quantification of the cell coverage of iba1-ir microglia. (**G**) Quantification of the area covered by GFAP-ir astrocytes in a frame of 0.2 mm × 0.2 mm in the ARC (illustrated in I) from each diet group (n = 6 for each group). (**H**) Quantification of the integrative intensity of CML-ir in a frame of 0.2 mm × 0.2 mm in the ARC (illustrated in J) from each diet group (n = 6 for each group). (**I**) Illustration of iba1-ir microglia in the ARC of each diet group; dark arrow pointed cells are magnified in the left upper corner. (**J**) Illustration of GFAP-ir astrocytes in the ARC of each diet group. (**K**) Illustration of CML-ir cells in the ARC of each diet group. III: third cerebral ventricle; Scale bar: 50 μm in I and K, and 100 μm in J. *P < 0.05, **P < 0.01, ***P < 0.001. Data are presented as means ± s.e.m. *P* values for 5-diet group-effects were analyzed by One-way ANOVA, followed by Student's *t* test for post-hoc analysis.

common AGE receptor (RAGE) (Figure 3A), and also to the activated leukocyte cell adhesion molecule (ALCAM) that shares the same genomic organization as RAGE in the gene fragment coding for the cytoplasmic domain [19]. In comparison to chow-fed mice, the HCHF diet fed mice had a significant increase of ALCAM and RAGE gene expression (Figure 3B).

By detecting the GFP that was incorporated in the construct for knocking out the RAGE gene ($RAGE^{-/-}$) or the ALCAM gene ($ALCAM^{-/-}$), we were able to examine the cell populations expressing these two receptors. Besides its known expression in endothelial cells [20], RAGE was exclusively expressed in every microglial cell (Figure 3C–F), but not in neuronal cells (including the POMC neurons; Supplementary Figure 6A and B) or astrocytes (Supplementary Figure 6C). Treating primary cultured hypothalamic microglia with CML significantly stimulated tumor necrosis factor alpha (TNFα) gene expression (Figure 3G). Consistently, infusion of CML into the mediobasal hypothalamic area for 6 h significantly increased iba1-ir microglia, identifying CML as a stimulatory factor for microglial reactivity (Figure 3H–J).

In contrast to RAGE, ALCAM was not expressed by microglia (Supplementary Figure 7A) and was only partially expressed by endothelial cells (Figure 3K and L). Also, ALCAM was not found on neurons (including CML-ir neurons, Supplementary Figure 7B and C) or the GFAP-ir astrocytes (Supplementary Figure 7D). Instead, ALCAM was intensely expressed by all the PDGFRβ-ir pericytes (Figure 3M and N). Pericytes are the major cell population expressing PDGFRβ. It is known that PDGF-B, the endogenous ligand of PDGFRβ, is highly expressed by

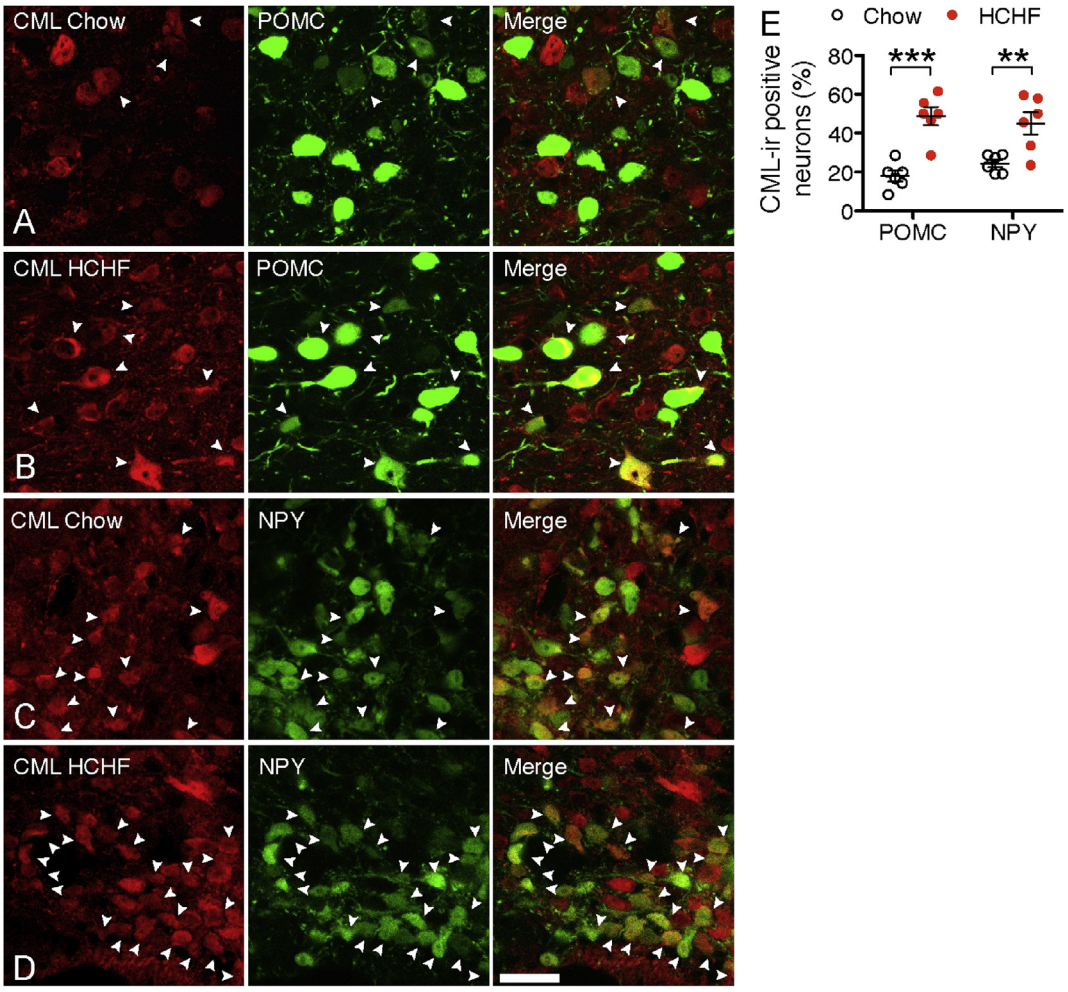

Figure 2: High carbohydrate, high fat diets increase CML production and secretion from hypothalamic neurons. (**A** & **B**) CML-ir POMC neurons in the ARC of mice on chow or HCHF diet. (**C** & **D**) CML-ir NPY neurons in the ARC of mice on chow or HCHF diet. (**E**) Quantification of the number of CML-ir POMC or NPY neurons (identified by *Pomc- or Npy*-driven e*GFP* labeling) in the ARC of mice on chow or HCHF ($n = 6$ mice for $POMC^{eGFP}$ or for NPY^{eGFP} on each diet, $P < 0.001$ for POMC, $P = 0.007$ for NPY). Scale bar: 30 μm. Data are presented as means ± s.e.m. $^{**}P < 0.01$, $^{***}P < 0.001$. *P* values for unpaired comparisons in were analyzed by two-tailed Student's *t* test.

microglia [21] and has an important role in regulating retinal capillary physiology [22]. These data indicate that CML might influence microglial PDGF-B production and, consequently, affect pericyte function via the PDGF-B receptor PDGFRβ. However, although we observed that CML stimulated TNFα gene expression in microglia, we did not see changes in PDGF-B gene expression (Figure 3F), indicating that PDGF-B might not be involved in microglial—pericyte interactions in the HCHF-diet condition.

3.4. Obesity and metabolic symptoms induced by a HCHF diet are improved in mice lacking functional RAGE and ALCAM genes

The evidence presented above suggests that under physiological conditions, CML secreted from neurons into the microenvironment in the mediobasal hypothalamus might be locally scavenged and taken up by microglia and/or pericytes. When the metabolic system is challenged by a HCHF diet, increased CML production by neurons requires a sufficient clearance by "supporting cells" in the microenvironment, in particularly the microglia and/or pericytes, these may exert stimulatory effects on the inflammatory response in microglia and/or pericytes, which, in turn, affect neuronal function and the control of energy metabolism.

To investigate whether RAGE and/or ALCAM mediates HCHF diet-induced microglial activation and angiopathy in obesity [2,4,23], we fed $RAGE^{-/-}$, $ALCAM^{-/-}$, or $RAGE\text{-}ALCAM^{-/-}$ mice a chow or HCHF diet (in all mice the HCHF started at 10 weeks of age) and examined their metabolic phenotype and hypothalamic inflammatory responses. On chow diet, $RAGE^{-/-}$, $ALCAM^{-/-}$ or $RAGE\text{-}ALCAM^{-/-}$ mice did not differ from their WT controls with respect to food intake and BW gain (Figure 4A—D and Figure 5A and B). When fed with HCHF diet, $RAGE^{-/-}$, $ALCAM^{-/-}$ and $RAGE\text{-}ALCAM^{-/-}$ mice had decreased food intake (Figure 4A and C and Figure 5A). BW gain was significantly reduced from wk14 to wk16 in $RAGE^{-/-}$ mice and in wk12 and from wk14 to wk16 in $ALCAM^{-/-}$ mice (Figure 4B and D). Interestingly, BW gain in $RAGE\text{-}ALCAM^{-/-}$ mice was already significantly lower than that in $RAGE\text{-}ALCAM^{+/+}$ mice by wk1 and continued through wk4 of the HCHF diet. This significant difference disappeared from wk6 to wk8, due to an increased BW gain in $RAGE\text{-}ALCAM^{-/-}$ mice but was present again from wk9 to wk16 (Figure 5B) and was associated with a lower fat and lean mass than in WT mice in wk16 (Figure 5C). Glucose tolerance did not differ between WT and $RAGE\text{-}ALCAM^{-/-}$ mice fed a chow diet (Figure 5D). In contrast, HCHF diet-induced glucose intolerance seen in WT mice was significantly improved in the RAGE-

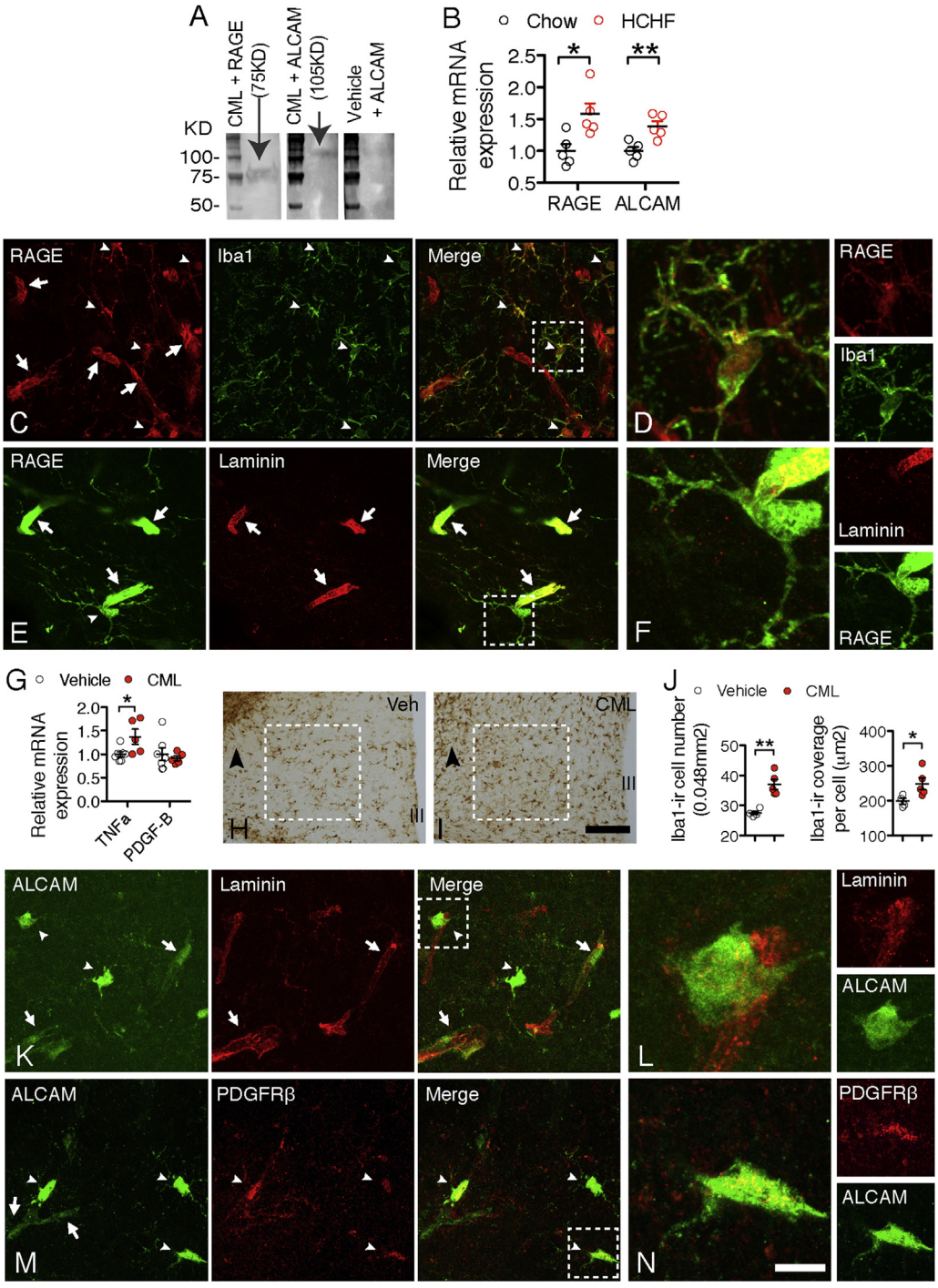

Figure 3: RAGE and ALCAM are expressed on non-neuronal cell populations. (**A**) CML binds to proteins of RAGE (molecular weight ≈ 75 KDa) and ALCAM (molecular weight ≈ 105 KDa); the vehicle does not bind to protein of either receptor, as illustrated by no band detected in binding of ALCAM. (**B**) RAGE and ALCAM gene expression in mediobasal hypothalami of chow or HCHF mice (n = 6 for chow or for HCHF, P = 0.019 for RAGE, P = 0.006 for ALCAM). (**C**) RAGE is intensely expressed by microglia (iba1-ir, indicated by white arrowheads). Higher magnifications of the areas framed by dashed lines are presented in **D**. (**E**) RAGE is intensely expressed on endothelial cells (laminin-ir, indicated by white arrows). Higher magnifications of the areas framed by dashed lines are presented in **F**. (**G**) CML stimulates TNFα, but not PDGF-B, gene expression in cultured primary microglia (n = 6 wells of cells for vehicle, n = 5 for TNFα treatments, P = 0.04 for TNFα). (**H & I**) CML stimulates microglial reactivity in the mediobasal hypothalamic area, arrowheads point to the areas where the tip of the infusion probes located. (**J**) Iba1-ir cell number and cell coverage in **H & I** (n = 4 mice for vehicle, n = 5 for CML). (**K**) ALCAM is expressed on part of the vasculature (laminin-ir, indicated by white arrows, two pericytes are indicated by white arrowheads); higher magnifications of the areas framed by dashed lines are presented in **L**. (**M**) ALCAM is expressed on pericytes (PDGFRβ-ir, white arrowheads). Higher magnifications of the areas framed by dashed lines are presented in **N**. Scale bar: 30 μm in C, E, K and M, 7.5um in D, F, L and N. Data are presented as means ± s.e.m. *P < 0.05, **P < 0.01. *P* values for unpaired comparisons were analyzed by two-tailed Student's *t* test.

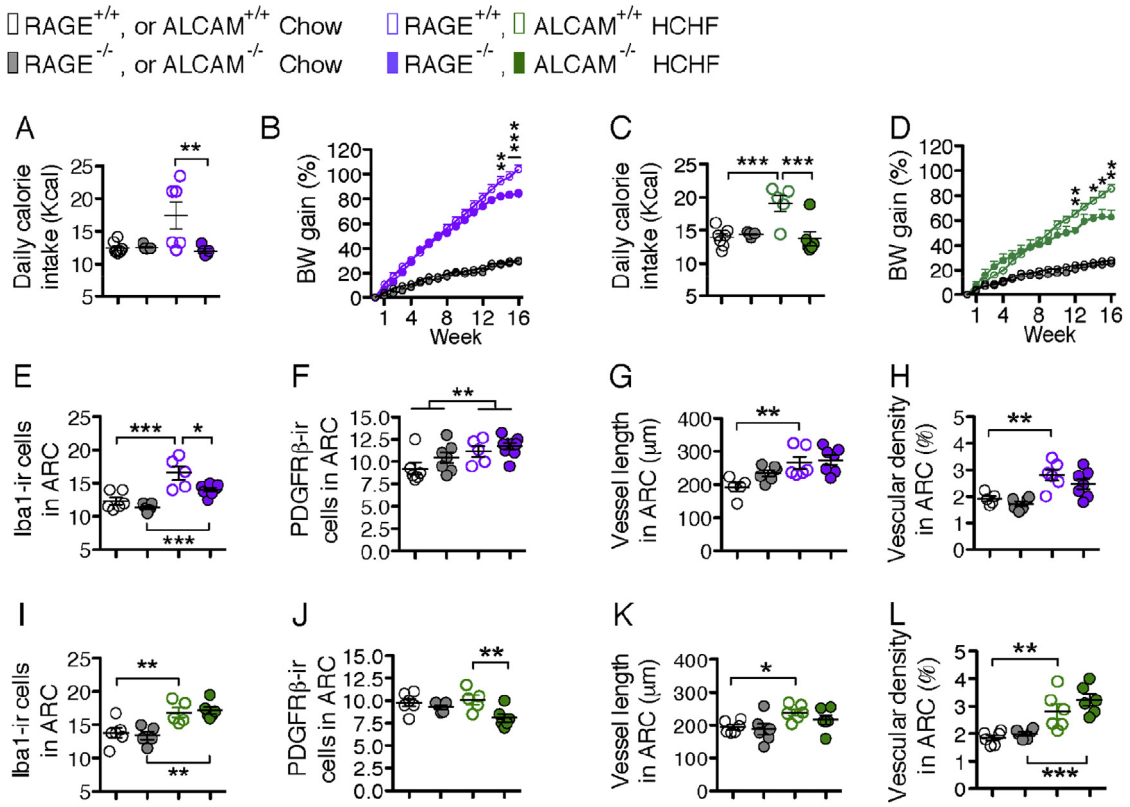

Figure 4: Deletions of RAGE or ALCAM genes improve metabolic symptoms induced by a HCHF diet and exert diverse impacts on microglia, pericytes, and vasculature in the arcuate nucleus. (**A** & **B**) Daily caloric intake (in wk10) and weekly BW gain of chow or HCHF diet-fed WT versus RAGE$^{-/-}$ mice (n = 5–8 per group); For weekly BW gain, in all time points, WT and RAGE$^{-/-}$ mice have less BW gain on chow diet than on HCHF diet ($P < 0.0001$); from wk14 to wk16, BW gain on HCHF of RAGE$^{-/-}$ mice is significantly less than WT mice. (**C** & **D**) Daily caloric intake (in wk10) and weekly BW gain of chow or HCHF diet fed WT mice versus ALCAM$^{-/-}$ mice (n = 5–8 per group). For weekly BW gain, from wk2 on, WT and ALCAM$^{-/-}$ mice have less BW gain in chow than in HCHF; from wk12, wk14 to wk16, BW-gain on HCHF of ALCAM$^{-/-}$ mice is significantly less than WT mice. (**E** & **F**) Quantification of the number of iba1-ir microglia and the PDGFRβ-ir pericytes in the ARC in chow or HCHF diet fed WT mice versus RAGE$^{-/-}$ mice (n = 5–9 per group). (**G & H**) Quantification of vessel length and vascular density in the ARC from chow or HCHF diet fed WT mice versus RAGE$^{-/-}$ mice (n = 5–7 per group). (**I** & **J**) Quantification of the number of iba1-ir microglia and the PDGFRβ-ir pericytes in the ARC in chow or HCHF diet fed WT mice versus ALCAM$^{-/-}$ mice (n = 5–6 per group). (**K & L**) Quantification of vessel length and vascular density in the ARC from chow or HCHF diet fed WT mice versus ALCAM$^{-/-}$ mice (n = 6 per group). Data are presented as means ± s.e.m. *$P < 0.05$, **$P < 0.01$, ***$P < 0.001$. Asterisks in B and D indicate significance between WT and RAGE$^{-/-}$ or ALCAM$^{-/-}$ mice on HCHF diet. Two-way ANOVA followed by Bonferroni multiple comparisons for post-hoc analysis was performed to detect significant interaction between genotype and diet on each parameter.

ALCAM$^{-/-}$ mice (Figure 5E). These data indicate that deletion of both RAGE and ALCAM genes was required to fully block the effects of AGEs on energy metabolism, while lack of either of these two genes only resulted in mild blockage effects.

3.5. Lacking RAGE and ALCAM prevents the hypothalamic inflammatory response and angiogenesis that occur on a HCHF diet

To determine whether lack of RAGE and/or ALCAM impacts microglia, pericytes, or the vasculature, we examined these cell populations in the ARC of RAGE$^{-/-}$, ALCAM$^{-/-}$ and RAGE-ALCAM$^{-/-}$ mice fed chow or HCHF diet. Consistent with previous findings [2,3,23], microglial cell number and cell coverage indicated by iba1-ir in the ARC was significantly increased on the HCHF diet in both WT and KO control group (Figure 4E, I and Figure 6A, B). In RAGE$^{-/-}$ mice, the number of iba1-ir cells in the ARC showed significant reduction relative to WT mice on the HCHF diet (Figure 4E) but remained significant higher than in the KO mice on chow diet, indicating that microglia reactivity is stimulated not only by the AGEs-RAGE pathway. No changes were apparent in ALCAM$^{-/-}$ mice on either diet (Figure 4I), but the increase in iba1-ir cell number did reach significance in the RAGE-ALCAM$^{-/-}$ mice fed HCHF diet (Figure 6A, F), although the iba1-ir cell coverage did not differ between the WT and RAGE-ALCAM$^{-/-}$ mice on HCHF diet. These data indicate that RAGE and ALCAM are direct or indirect mediators of CML (and other AGE species) action on microglial reactivity, and that deletion of both receptors can effectively block the HCHF diet-induced microglial activation.

In RAGE$^{-/-}$ mice, the number of PDGFRβ-ir cells increased from chow to HCHF diet, indicating that pericytes were activated upon taking up CML (and other AGE species). In ALCAM$^{-/-}$ mice, the number of PDGFRβ-ir cells decreased from WT to KO in HCHF diet fed mice, indicating lack of ALCAM can decrease pericytes activity on a HCHF diet. In RAGE-ALCAM$^{-/-}$ mice, the number of PDGFRβ-ir cells decreased from WT to KO mice, indicating that the lack of both RAGE and ALCAM reduces pericyte activity in chow and HCHF fed conditions (Figure 4F, J and Figure 6C and G).

From a canonical view, RAGE and/or ALCAM expressed by endothelial cells are responsible for taking up CML (and other AGE species) from the circulation. In the mediobasal hypothalamus, the intense interaction between neurons, glia and vasculature raises the possibility that CML produced locally may act on endothelial cells. We examined vessel length based on the previous observation that HCHF diets can induce neovasculature formation [4]. In all WT mice, increased vessel

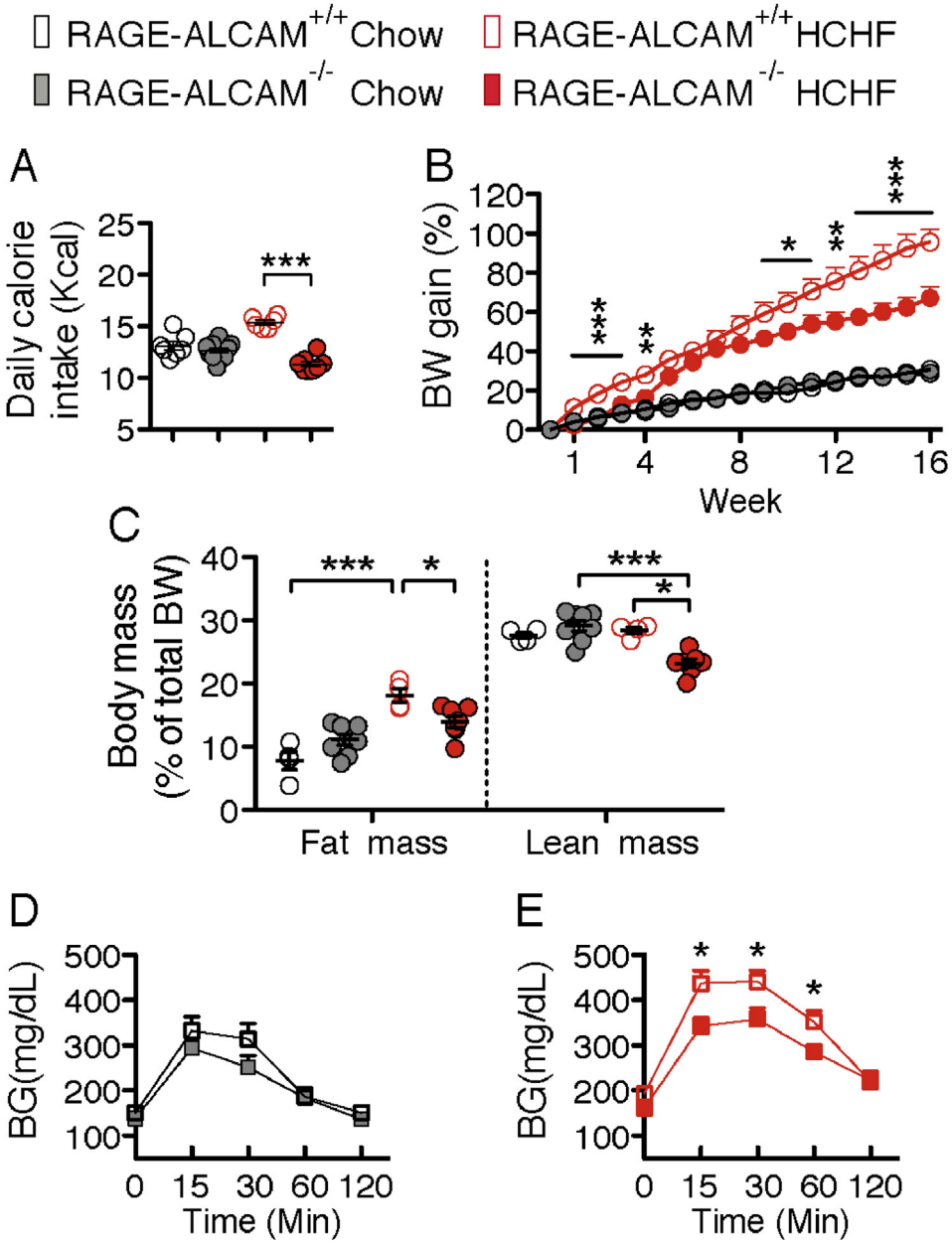

Figure 5: Deletion of RAGE and ALCAM genes improves metabolic symptoms induced by a HCHF diet. (**A** & **B**) Daily caloric intake (in wk10) and weekly body weight gain of chow or HCHF diet-fed WT versus RAGE-ALCAM$^{-/-}$ mice (n = 6–11 per group); for weekly BW gain, from wk5 on, WT and RAGE-ALCAM$^{-/-}$ mice have less BW gain in chow than in HCHF; From wk1 to wk4 and from wk9 to wk16, there are significant effect of genotype on BW gain on HCHF. (**C**) Body composition of WT versus RAGE-ALCAM$^{-/-}$ mice fed HCHF diet (n = 4–8 per group). (**D**) Glucose tolerance of WT versus RAGE-ALCAM$^{-/-}$ mice fed chow or HCHF diet (n = 5–7 per group). (**E**) Glucose tolerance of RAGE-ALCAM$^{-/-}$ mice fed chow or HCHF diet (n = 5–7 per group). Data are presented as means ± s.e.m. *P < 0.05, **P < 0.01, ***P < 0.001. Asterisks indicate significance between WT and RAGE-ALCAM$^{-/-}$ mice. Two-way ANOVA followed by Bonferroni multiple comparisons for post-hoc analysis was performed to detect significant interactions between genotype and diet on daily caloric intake, BW gain and body mass. Two-tailed Student's *t* test was performed between each time point in D and E, to detect the effect of genotype on glucose tolerance on chow or HCHF diet.

length and vascular density were apparent in all the HCHF groups (Figure 4G, H, K, L and Figure 6D, E, H, I). These increases were completely abolished in RAGE-ALCAM$^{-/-}$ mice, indicating that RAGE and ALCAM coordinately mediate the CML action on vasculature.

4. DISCUSSION

Regarding the respective roles of fat and carbohydrate in hypercaloric environment-induced obesity, there is evidence to suggest that high-fat diets, particularly diets containing saturated fats [24], promote obesity and the associated metabolic syndrome. Evidence indicating a pivotal role for high sugar diets has also been presented [25], but remains controversial [26]. The present experiments provide clear evidence that the amount of carbohydrate in a diet determines whether a high-fat diet will induce obesity, or not.

The HCHF diet induced microglial activation is likely due to resident microglial proliferation, since a recent study on hypothalamic inflammation showed that microglia expansion in the hypothalamus requires

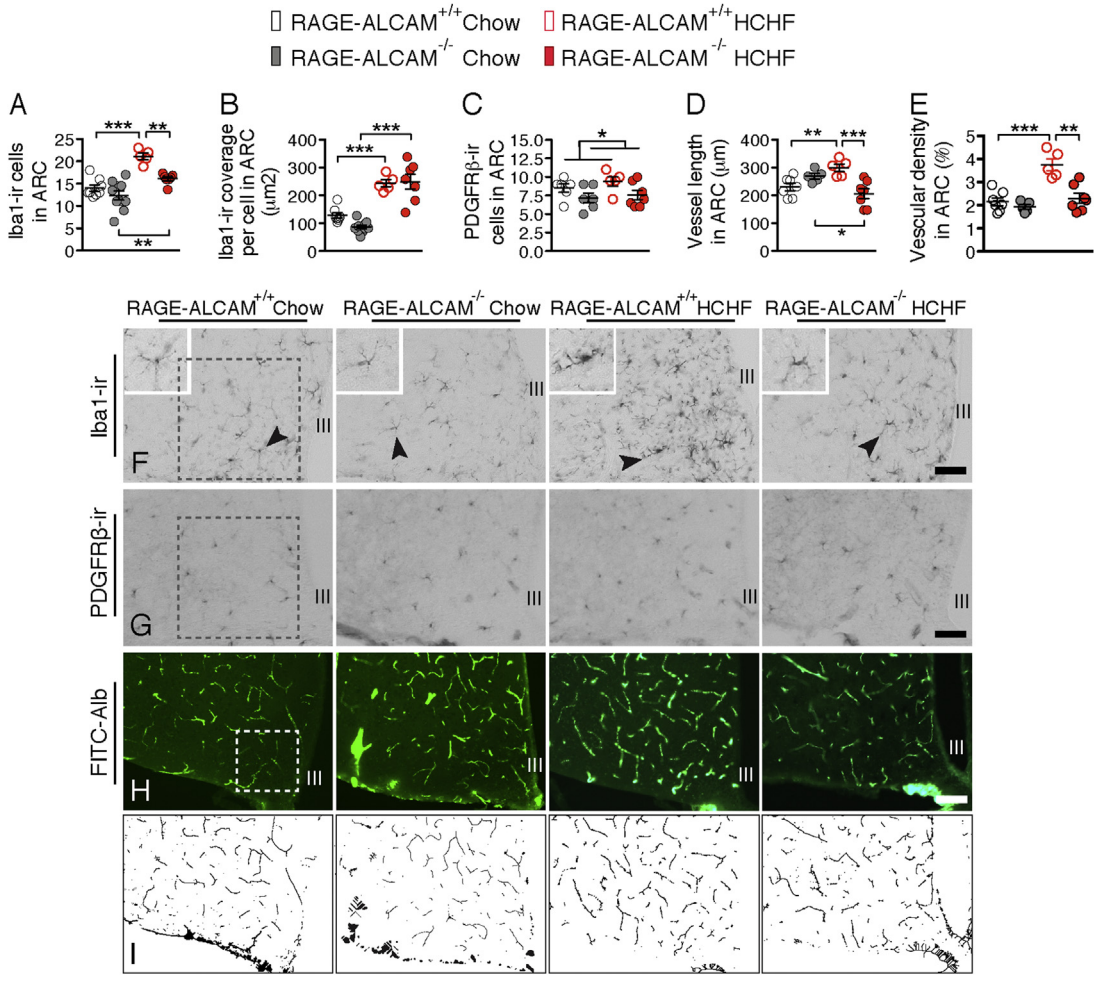

Figure 6: Deletion of RAGE and ALCAM genes reduces microglial reactivity and neovasculature formation in the arcuate nucleus (**A, B** & **C**) Quantification of iba1-ir microglial number, coverage and the PDGFRβ-ir pericytes number in the ARC from chow or HCHF diet fed WT (n = 5—8 per group) versus RAGE-ALCAM$^{-/-}$ mice (n = 7—10 per group). (**D & E**) Quantification of vessel length and vascular density in the ARC from chow or HCHF diet fed WT (n = 5—7 per group) versus RAGE-ALCAM$^{-/-}$ mice (n = 5—7 per group). (**F—H**) Illustrations of the iba1-ir microglia, PDGFRβ-ir pericytes and FITC-albumin labeled vessels in WT versus RAGE-ALCAM$^{-/-}$ mice fed chow or HCHF diet, with a frame of 0.2 mm × 0.2 mm for quantifications in the ARC. (**I**) Illustration of the skeletonization of vessel in H for vascular density analysis. III: third cerebral ventricle. Scale bar: 50um in F and G, 100um in F. Data are presented as means ± s.e.m. *P < 0.05, **P < 0.01, ***P < 0.001. Two-way ANOVA followed by Bonferroni multiple comparisons for post-hoc analysis was performed to detect significant interaction between genotype and diet on each parameter.

the adequate presence of both fats and carbohydrates, a very high-fat with very low-carbohydrate diet did not affect microglial proliferation [27].

The obesity induced by HCHF diets was associated with a significant increase of microglial reactivity and CML content in POMC and NPY neurons. Because the two receptors that can bind CML are not expressed by neurons but are expressed by microglia and endothelial cells or pericytes, we conclude that in the local microenvironment, microglia, pericytes, and endothelial cells are the CML (and other AGEs species)-responsive cells. This conclusion is supported by the reduction of reactivity in microglia and pericytes, and the reduced neovasculature formation in the hypothalamic ARC of RAGE and ALCAM knockout mice fed a HCHF diet. The concurrent amelioration of HCHF-induced obesity and metabolic disorders suggests that CML might be one of the key mediators of HCHF diet-induced obesity via a medi-obasal hypothalamic inflammatory response governed by microglia in association with pericytes and vasculature.

Our data suggest that different high fat diets generate different levels and types of AGEs. In a previous study on RAGE regulating metabolic and inflammatory responses to a high fat diet, genetic deletion of the RAGE gene largely prevented a lard based 60% high fat diet-induced obesity [28]. This indicates that certain amounts and types of AGEs probably act selectively on either RAGE or ALCAM. Future studies are needed to understand how each type of AGE interacts with RAGE and/or ALCAM.

CML produced by lipid peroxidation and non-enzymatic glycoxidation reactions is considered an oxidative stress marker [29]. A previous study reported that oxidative stress-induced reactive oxygen species (ROS) are elevated in diet-induced obese mouse POMC and NPY/AgRP neurons [30]. In the current study, we also observed CML in both POMC and NPY neurons. However, the fact that receptors for CML binding are not expressed by neurons, but are highly expressed by microglia and/or pericytes, indicates that for maintaining a healthy microenvironment, the so-called glial-vascular supporting unit may be an important initial step in helping neurons to clean up metabolic debris. Studies in peripheral tissues, including liver and vessels, report a similar mechanism; i.e., the cells that take up AGEs are mainly endothelial cells and macrophages [31,32].

Under physiological conditions, the immune response of microglia may be sufficient to clear away most of the neuronal debris. However, in the HCHF diet condition, the overload of lipids and glucose from the diet results in excessive CML (and other AGE species) production in neurons, the excessive amount of CML taken up by microglia will concurrently increase microglial reactivity. It is likely that in the local microenvironment, microglia are not the only cells able to take up CML; the ALCAM-expressing pericytes may also play a role. As an essential component of neurovasculature the role of pericytes in maintaining internal brain homeostasis has gained more and more attention since these cells were found to express the macrophage scavenger receptor [33] and to be important players in the pro-inflammatory response of the brain to an immune challenge [34,35]. In the present study, the identification of pericytes as a group of cells able to take up CML confirmed the immune property of pericytes [36].

In the diet-induced obese mouse hypothalamus, astrocytosis has been considered to be part of the hypothalamic inflammatory response to a hypercaloric diet. We found that astrocytosis was mainly a response to the fat but not to the carbohydrate content of the diet and was not correlated to the dietary-induced changes in food intake and BW, indicating that astrocytic activity might mainly be determined by lipid metabolism. This concept also nicely fits with the fact that astrocytes are considered to be the major source of ketone body production in the brain [37].

Based on the current evidence, we propose that endothelial cells, in addition to taking up the CML (and other AGE species) through RAGE, can also accomplish this via ALCAM. When CML and other AGE species are increased as a result of HCHF diet consumption, endothelial cells need to enhance their uptake capacity. In the long run, this increasing amount of CML (and other AGE species) may cause endothelial cellular dysfunction and lead to neovasculature formation in the hypothalamic ARC in HCHF diet-induced obesity, as we have reported in our previous study [4]. The present findings demonstrate that RAGE and ALCAM signaling pathways mediate the angiopathy effects of a HCHF diet in the hypothalamic ARC via CML and other AGE species. In line with our findings, other studies have observed that in diabetic retinopathy, an accumulation of CML around vessels in the retina was associated with vascular endothelial growth factor (VEGF), suggesting that CML could also play a role in VEGF expression in retinopathy and associated microvascular complications [38].

We propose a model for the hypothalamic neuron-glia-vascular unit in which, under physiological conditions, a basal level of CML (and other AGE species)-modified macromolecules is secreted by neurons into the interstitial space, and microglia are the primary cells responsible for cleaning up these CML-modified macromolecules. The perivascular pericytes most likely play a substitutive role in assisting microglia and endothelial cells to take up the excessive amounts of modified CML macromolecules. When, driven by a HCHF diet, CML (and other AGE species) are over-produced in neurons, and the uptake of CML-modified macromolecules is enhanced in microglia. This results in microglial activation and production of more TNFα, by RAGE signaling, that subsequently reinforces microglial activity and the inflammatory response. In addition, through ALCAM signaling, this may also lead to pericyte reactivity. Thus, in the local microenvironment, a dynamic clearance system for neuronal debris is developed by microglia and pericytes.

5. CONCLUSIONS

Calorie restriction is one of the major approaches to combat obesity and its associated metabolic disorders. The evidence we provide here indicates that restricting dietary fat is not the only factor that needs to be considered for body weight reduction in obese individuals and that dietary carbohydrates might substantially gate the efficiency of calorie restriction for body weight reduction, via a hypothalamic mechanism. Furthermore, it is known that inflammatory mechanisms play a crucial role in neurodegenerative disorders and that the elimination of dietary carbohydrates exerts a neuro-protective effect by alleviating symptoms in Alzheimer's and Parkinson's disease [39,40]. Whether the neuro-protective effects of low carbohydrate diets in these pathologies are also mediated by microglial mechanisms needs to be explored in future studies.

ACKNOWLEDGMENTS

T.F. and P.N. are supported by Deutsche Forschungsgemeinschaft (DFG; SFB1118) and Dietmar Hopp Foundation (DHS). R.J.S. was supported by Ethicon Endo-Surgery/ Johnson & Johnson, Novo Nordisk, Daiichi Sankyo, Janssen/Johnson & Johnson, Novartis, Nestle, Takeda, Boehringer-Ingelheim and Sanofi. M.H.T. is supported by the Alexander von Humboldt Foundation, the Helmholtz Alliance ICEMED and the Helmholtz Initiative on Personalized Medicine iMed by Helmholtz Association, the Helmholtz cross-program topic 'Metabolic Dysfunction', the German Research Foundation DFG (SFB1123 & Nutripathos Project ANR- 15-CE14-0030) as well as the European Research Council ERC (AdG HypoFlam no. 695054). C.X.Y. is supported by *AMC fellowship (2014)* and Dutch Diabetes Fonds (2015.82.1826), The Netherlands.

CONFLICT OF INTEREST

The authors declare that there is no conflict of interest that could be perceived as prejudicing the impartiality of the research reported.

APPENDIX A. SUPPLEMENTARY DATA

Supplementary data related to this article can be found at http://dx.doi.org/10.1016/j.molmet.2017.06.008.

REFERENCES

[1] Kalin, S., Heppner, F.L., Bechmann, I., Prinz, M., Tschop, M.H., Yi, C.X., 2015. Hypothalamic innate immune reaction in obesity. Nature Reviews Endocrinology 11:339–351.

[2] Thaler, J.P., Yi, C.X., Schur, E.A., Guyenet, S.J., Hwang, B.H., Dietrich, M.O., et al., 2012. Obesity is associated with hypothalamic injury in rodents and humans. Journal of Clinical Investigation 122:153–162.

[3] De Souza, C.T., Araujo, E.P., Bordin, S., Ashimine, R., Zollner, R.L., et al., 2005. Consumption of a fat-rich diet activates a proinflammatory response and induces insulin resistance in the hypothalamus. Endocrinology 146:4192–4199.

[4] Yi, C.X., Gericke, M., Kruger, M., Alkemade, A., Kabra, D.G., Hanske, S., et al., 2012. High calorie diet triggers hypothalamic angiopathy. Molecular Metabolism 1:95–100.

[5] Milanski, M., Degasperi, G., Coope, A., Morari, J., Denis, R., Cintra, D.E., et al., 2009. Saturated fatty acids produce an inflammatory response predominantly through the activation of TLR4 signaling in hypothalamus: implications for the pathogenesis of obesity. Journal of Neuroscience 29:359–370.

[6] Liliensiek, B., Weigand, M.A., Bierhaus, A., Nicklas, W., Kasper, M., Hofer, S., et al., 2004. Receptor for advanced glycation end products (RAGE) regulates sepsis but not the adaptive immune response. Journal of Clinical Investigation 113:1641–1650.

[7] Saura, J., Tusell, J.M., Serratosa, J., 2003. High-yield isolation of murine microglia by mild trypsinization. Glia 44:183–189.

[8] Wu, Y., Li, Q., Chen, X.Z., 2007. Detecting protein-protein interactions by Far western blotting. Nature Protocols 2:3278–3284.

[9] Knittelfelder, O.L., Weberhofer, B.P., Eichmann, T.O., Kohlwein, S.D., Rechberger, G.N., 2014. A versatile ultra-high performance LC-MS method for lipid profiling. Journal of Chromatography B, Analytical Technologies in the Biomedical and Life Sciences 951–952:119–128.

[10] Mobbs, C.V., Mastaitis, J., Yen, K., Schwartz, J., Mohan, V., Poplawski, M., et al., 2007. Low-carbohydrate diets cause obesity, low-carbohydrate diets reverse obesity: a metabolic mechanism resolving the paradox. Appetite 48: 135–138.

[11] Bielohuby, M., Menhofer, D., Kirchner, H., Stoehr, B.J., Muller, T.D., Stock, P., et al., 2011. Induction of ketosis in rats fed low-carbohydrate, high-fat diets depends on the relative abundance of dietary fat and protein. American Journal of Physiology — Endocrinology and Metabolism 300:E65–E76.

[12] Zengin, A., Kropp, B., Chevalier, Y., Junnila, R., Sustarsic, E., Herbach, N., et al., 2016. Low-carbohydrate, high-fat diets have sex-specific effects on bone health in rats. European Journal of Nutrition 55:2307–2320.

[13] Shai, I., Schwarzfuchs, D., Henkin, Y., Shahar, D.R., Witkow, S., Greenberg, I., et al., Dietary Intervention Randomized Controlled Trial, G, 2008. Weight loss with a low-carbohydrate, Mediterranean, or low-fat diet. The New England Journal of Medicine 359:229–241.

[14] Klein, P., Tyrlikova, I., Mathews, G.C., 2014. Dietary treatment in adults with refractory epilepsy: a review. Neurology 83:1978–1985.

[15] Levick, S.P., Loch, D.C., Taylor, S.M., Janicki, J.S., 2007. Arachidonic acid metabolism as a potential mediator of cardiac fibrosis associated with inflammation. Journal of Immunology 178:641–646.

[16] Singh, R., Barden, A., Mori, T., Beilin, L., 2001. Advanced glycation end-products: a review. Diabetologia 44:129–146.

[17] Requena, J.R., Fu, M.X., Ahmed, M.U., Jenkins, A.J., Lyons, T.J., Thorpe, S.R., 1996. Lipoxidation products as biomarkers of oxidative damage to proteins during lipid peroxidation reactions. Nephrology Dialysis Transplantation 11(Suppl. 5):48–53.

[18] Huttunen, H.J., Fages, C., Rauvala, H., 1999. Receptor for advanced glycation end products (RAGE)-mediated neurite outgrowth and activation of NF-kappaB require the cytoplasmic domain of the receptor but different downstream signaling pathways. Journal of Biological Chemistry 274:19919–19924.

[19] Sessa, L., Gatti, E., Zeni, F., Antonelli, A., Catucci, A., Koch, M., et al., 2014. The receptor for advanced glycation end-products (RAGE) is only present in mammals, and belongs to a family of cell adhesion molecules (CAMs). PLoS One 9:e86903.

[20] Schmidt, A.M., Hasu, M., Popov, D., Zhang, J.H., Chen, J., Yan, S.D., et al., 1994. Receptor for advanced glycation end products (AGEs) has a central role in vessel wall interactions and gene activation in response to circulating AGE proteins. Proceedings of the National Academy of Sciences of the United States of America 91:8807–8811.

[21] Zhang, Y., Chen, K., Sloan, S.A., Bennett, M.L., Scholze, A.R., O'Keeffe, S., et al., 2014. An RNA-sequencing transcriptome and splicing database of glia, neurons, and vascular cells of the cerebral cortex. Journal of Neuroscience 34: 11929–11947.

[22] Forsberg-Nilsson, K., Erlandsson, A., Zhang, X.Q., Ueda, H., Svensson, K., Nister, M., et al., 2003. Oligodendrocyte precursor hypercellularity and abnormal retina development in mice overexpressing PDGF-B in myelinating tracts. Glia 41:276–289.

[23] Gao, Y., Ottaway, N., Schriever, S.C., Legutko, B., Garcia-Caceres, C., de la Fuente, E., et al., 2014. Hormones and diet, but not body weight, control hypothalamic microglial activity. Glia 62:17–25.

[24] Vessby, B., 2003. Dietary fat, fatty acid composition in plasma and the metabolic syndrome. Current Opinion in Lipidology 14:15–19.

[25] Dhingra, R., Sullivan, L., Jacques, P.F., Wang, T.J., Fox, C.S., Meigs, J.B., et al., 2007. Soft drink consumption and risk of developing cardiometabolic risk factors and the metabolic syndrome in middle-aged adults in the community. Circulation 116:480–488.

[26] Stanhope, K.L., 2016. Sugar consumption, metabolic disease and obesity: the state of the controversy. Critical Reviews in Clinical Laboratory Sciences 53: 52–67.

[27] Andre, C., Guzman-Quevedo, O., Rey, C., Remus-Borel, J., Clark, S., Castellanos-Jankiewicz, A., et al., 2017. Inhibiting microglia expansion prevents diet-induced hypothalamic and peripheral inflammation. Diabetes 66:908–919.

[28] Song, F., Hurtado del Pozo, C., Rosario, R., Zou, Y.S., Ananthakrishnan, R., Xu, X., et al., 2014. RAGE regulates the metabolic and inflammatory response to high-fat feeding in mice. Diabetes 63:1948–1965.

[29] Fu, M.X., Requena, J.R., Jenkins, A.J., Lyons, T.J., Baynes, J.W., Thorpe, S.R., 1996. The advanced glycation end product, Nepsilon-(carboxymethyl)lysine, is a product of both lipid peroxidation and glycoxidation reactions. Journal of Biological Chemistry 271:9982–9986.

[30] Diano, S., Liu, Z.W., Jeong, J.K., Dietrich, M.O., Ruan, H.B., Kim, E., et al., 2011. Peroxisome proliferation-associated control of reactive oxygen species sets melanocortin tone and feeding in diet-induced obesity. Nature Medicine 17:1121–1127.

[31] Svistounov, D., Oteiza, A., Zykova, S.N., Sorensen, K.K., McCourt, P., McLachlan, A.J., et al., 2013. Hepatic disposal of advanced glycation end products during maturation and aging. Experimental Gerontology 48:549–556.

[32] Kirstein, M., Brett, J., Radoff, S., Ogawa, S., Stern, D., Vlassara, H., 1990. Advanced protein glycosylation induces transendothelial human monocyte chemotaxis and secretion of platelet-derived growth factor: role in vascular disease of diabetes and aging. Proceedings of the National Academy of Sciences of the United States of America 87:9010–9014.

[33] Balabanov, R., Beaumont, T., Dore-Duffy, P., 1999. Role of central nervous system microvascular pericytes in activation of antigen-primed splenic T-lymphocytes. Journal of Neuroscience Research 55:578–587.

[34] Persidsky, Y., Hill, J., Zhang, M., Dykstra, H., Winfield, M., Reichenbach, N.L., et al., 2016. Dysfunction of brain pericytes in chronic neuroinflammation. Journal of Cerebral Blood Flow and Metabolism 36:794–807.

[35] Guijarro-Munoz, I., Compte, M., Alvarez-Cienfuegos, A., Alvarez-Vallina, L., Sanz, L., 2014. Lipopolysaccharide activates Toll-like receptor 4 (TLR4)-mediated NF-kappaB signaling pathway and proinflammatory response in human pericytes. Journal of Biological Chemistry 289:2457–2468.

[36] Kamouchi, M., Ago, T., Kitazono, T., 2011. Brain pericytes: emerging concepts and functional roles in brain homeostasis. Cellular and Molecular Neurobiology 31:175–193.

[37] Blazquez, C., Woods, A., de Ceballos, M.L., Carling, D., Guzman, M., 1999. The AMP-activated protein kinase is involved in the regulation of ketone body production by astrocytes. Journal of Neurochemistry 73:1674–1682.

[38] Murata, T., Nagai, R., Ishibashi, T., Inomuta, H., Ikeda, K., Horiuchi, S., 1997. The relationship between accumulation of advanced glycation end products and expression of vascular endothelial growth factor in human diabetic retinas. Diabetologia 40:764–769.

[39] Reger, M.A., Henderson, S.T., Hale, C., Cholerton, B., Baker, L.D., Watson, G.S., et al., 2004. Effects of beta-hydroxybutyrate on cognition in memory-impaired adults. Neurobiology of Aging 25:311–314.

[40] Jabre, M.G., Bejjani, B.P., 2006. Treatment of Parkinson disease with diet-induced hyperketonemia: a feasibility study. Neurology 66:617 [author reply 617].

